

## A SUPERCONDUCTING RING-CYCLOTRON FOR PROTON THERAPY

H.N. JUNGWIRTH, J.G. DE VILLIERS, A.H. BOTHA, A. MÜLLER, W.A.G. NEL,  
L.K.O. SCHÜLEIN and H.A. SMIT

National Accelerator Centre, P.O. Box 72, Faure 7131, South Africa

A new type of superconducting ring-cyclotron (SRC) with split sector magnets is proposed for dedicated proton therapy installations. The SRC is a fixed frequency machine with a small internal ion source and combines the advantages of conventional superconducting cyclotrons with the accessibility and ease of extraction characteristic of separated-sector cyclotrons. With variable-radius extraction, the SRC could provide external proton beams from ~100 MeV up to 220 MeV for direct use in scanning systems without prior energy degradation. The characteristics of the proposed cyclotron are examined, and the results of investigations into the design of the magnet configuration and rf-resonators are presented and discussed.

### 1 Introduction

The number of cyclotrons with proton energies between 200 and 250 MeV proposed for hospital-based radiotherapy facilities has increased substantially in recent years.<sup>1-4</sup> Both room-temperature and superconducting design versions have been drafted, and the first of these cyclotrons is now under construction.<sup>5,6</sup> Such machines are compact in size, and designed to operate with a small internal ion source for delivering proton beams of high quality and abundant intensity at a fixed energy. The latter is dictated by the unacceptable complexity, both in hardware and operation, which would result from providing energy variability with these cyclotrons, while the energy of the extracted beam can be reduced by a suitable energy degrader.

In contrast, synchrotrons need an additional injector and deliver pulsed beams of marginal intensity, but almost inherently and instantaneously (pulse to pulse) can provide variable energies. Their external beam quality is more than adequate when the well-established scattering method is used for treating the patients, whereas cyclotrons could also provide the pencil beams required for spot scanning which is currently being developed at PSI.<sup>7</sup> The expected advantages of this new modality in proton therapy rely on the improved precision of the dose distribution which can be achieved both laterally and in depth.

The SRC discussed in this paper is a new type of superconducting cyclotron which could provide significant advantages over existing proposals for such applications, in particular with regard to beam extraction and energy variability. Its concept is based on a sector magnet design employing S-coils<sup>8</sup>, and offers a compact machine with low operating costs in combination with the accessibility and extraction efficiency which are characteristic of separated-sector and ring cyclotrons. The aim of our studies is to establish the design characteristics of such a machine, and the results obtained thus far are presented here.

### 2 Cyclotron Characteristics

The proposed SRC layout is adopted from our existing 200 MeV separated-sector cyclotron (SSC) at NAC and shown in Figure 1. The main components are the four 24-ton sector magnets and two 106 MHz  $\lambda/2$  rf-resonators, fitting into a common octagonal vacuum chamber of ~4.6 m diameter and 3 m height. Each sector magnet features two pole plates at room temperature and a separate cryostat containing the superconducting coils together with the flux-return yoke. The four cryostats and the main compartment of the vacuum chamber have to be pumped down and vented independently. Also indicated schematically are an extraction system similar to the one used in our SSC, and beam diagnostic equipment outside the central region.

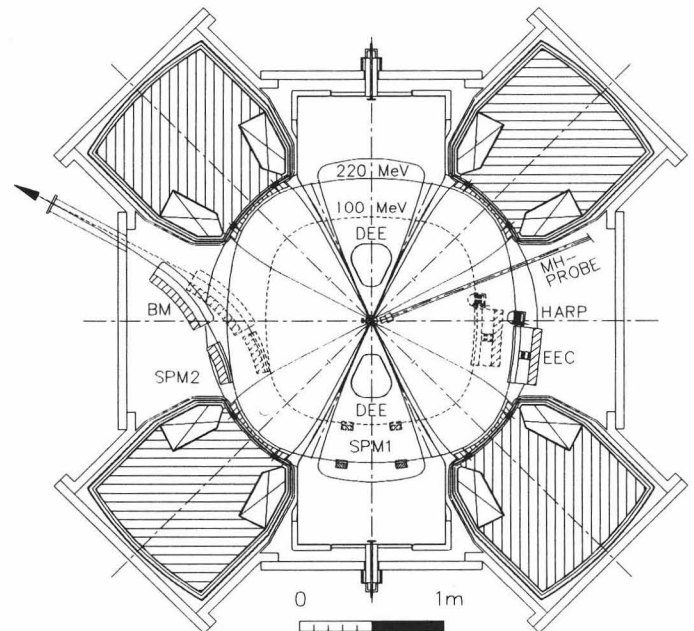


Figure 1: The proposed superconducting ring-cyclotron layout.

The two rf-resonators operate in phase at the 4th harmonic of the orbital rotation frequency of the beam, and the magnetic field in the cyclotron centre is close to 1.74 tesla. The resonators should be designed such that the peak acceleration voltage increases from  $\geq 40$  kV in the central region to  $\geq 240$  kV at full radius, thus limiting the number of turns in the SRC to  $\sim 300$  and providing strong phase compression of the beam to improve the extraction efficiency. The mean orbit radius for 220 MeV protons is 1.056 m and requires an average field of almost 2.15 tesla.

The radial field shape is determined by isochronism which must be maintained with very high accuracy ( $\delta B/B < 5 \times 10^{-5}$ ) and inherently yields good radial beam focusing. The azimuthal field shape has to provide sufficient vertical beam focusing to overcome the defocusing effect of the radial field increase. In order to achieve this in a  $4 \times 34^\circ$  sector geometry without spiral, the field on the 220 MeV proton orbit must typically vary from 4.2 tesla in the pole gap of the magnets to 0.9 tesla in the valleys, and superconducting coils are necessary to produce such fields without excessive power consumption.

The relatively low magnetic field in the valleys permits the efficient and reliable use of conventional electric and magnetic extraction devices, although at least some of the latter would have to be augmented with permanent magnets to provide the basic field reversal required relative to the main guiding field. A radial adjustment of less than 0.3 m is sufficient for the extraction components to cover the proton energy range from 100 to 220 MeV. Such energy changes could be accomplished in 10 to 20 minutes, required for repositioning and tuning the extraction components, because very little other retuning of the machine should be necessary.

### 3 Sector Magnets

The magnet design is similar to the one proposed originally for such a SRC<sup>8</sup>, but makes provision for supporting the substantial magnetic forces acting on the S-coils without conducting excessive heat through the cryostat walls into the liquid He bath at 4.2 K. For this purpose the magnets are split at the radial boundary of each sector, so that its flux-return yoke can be included in the cryostat as shown in Figure 1. Figure 2 illustrates the result of a two-dimensional field computation for such a magnet geometry. The magnetic attraction between the poles and coil armature counteracts the resultant magnetic force pushing the S-coils in radial direction. Also the efficiency of the magnet design is improved in this way, and the flux penetration into the coils is reduced as far as possible.

With a suitable choice of the geometry and excitation of the S-coils, the required radial and azimuthal field shape

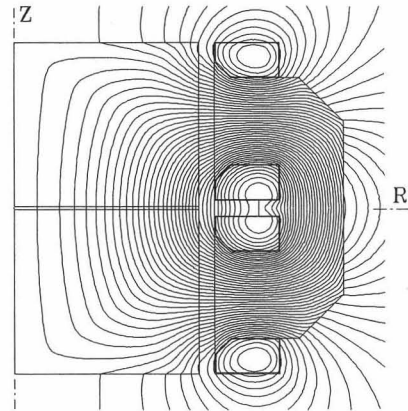


**Figure 2:** The flux plot computed for a radial section of a SRC magnet assuming rotational symmetry about the z-axis.

can be produced using a constant pole gap of 20 mm, without the need for trim-coils or excessive shimming. The magnet geometry shown in Figure 1 was designed by making use of the TOSCA codes<sup>9</sup>, and is based on an excitation of 3.04 MA turns per coil with a mean current density of less than 38 A/mm<sup>2</sup>, thus facilitating cryostable operation. Without this restriction, the current density could be increased safely up to 60 A/mm<sup>2</sup> in practice<sup>10</sup>, leading to a considerably more efficient and cost-effective design (smaller coils and less iron). A gap of 30 mm is assumed between the coil armature and the radial rim of the pole plates to provide ample space for inserting an intermediate heat shield.

The resulting sector magnets are 3 m high and have a total iron mass of 96 metric tons. The azimuthal pole width decreases gradually from 34° at 0.7 m radius to 27.5° at the pole radius of 1.15 m, thus adding precious space in the valleys and increasing the vertical focusing of the beam near extraction by a factor 2 ( $v_z \geq 0.2$ ). In the central region, the apices of the magnet sectors are cut back both radially and azimuthally to provide space for the ion source and resonator tips, but the central field can be maintained and shaped as required using symmetric iron plugs with a radius of 40 mm in addition to the remaining parts of the sectors. The conical plugs leave a gap of 70 mm at the expected position of the ion source.

The field computed with TOSCA is isochronous within 0.2% up to the 220 MeV equilibrium orbit and has good focusing properties. The stored energy is 70 MJ at full excitation, and the maximum field across the superconductors does not exceed 6.4 tesla which allows the use of standard NbTi cables with a Cu matrix in a liquid He bath at 4.2 K. Calculations show that each pair of S-coils is pushed radially away from the cyclotron axis with a maximum force of 6.3 MN, while the S-coil armature is anchored to the poles with 13.3 MN. This leaves a net

retaining force of  $\sim 7$  MN which can be supported mechanically by struts bracing the four magnet yokes against each other. Also the potted coil structure must have sufficient strength to prevent relative conductor movements which could lead to quenches. The larger cryomass may require longer cool-down periods up to 1 month, but helps to stabilize the temperature during operation.

#### 4 Rf-Resonators

The rf-system works at a fixed frequency of 106 MHz (FM broadcasting range). By using trimmers provision is made for  $\sim 2\%$  frequency adjustment. The two resonators have triangular ( $\sim 47^\circ$ ) dees operating in phase, and are located in opposite valleys between the sector magnets. Each dee is driven by a master oscillator power amplifier system and has its own phase and amplitude stabilization feedback loops. A phase stability of  $< 1^\circ$  is required between the dees to limit the relative variation in acceleration voltage to  $1 \times 10^{-4}$ . For single turn extraction, the amplitude stability should be better than  $5 \times 10^{-4}$  which is easily achieved. The power amplifiers are placed near the resonators and capacitively coupled to the dees. The power tubes will operate with an anode impedance of the order of  $500 \Omega$ . The total power consumption should not exceed 150 kW per resonator.

For designing the resonator we used a parametrized transmission-line representation of the geometry which was progressively improved and refined. In such a representation, the resonator circuit consists of many short transmission-line sections, with different impedances, which are connected in series or parallel as is required, and terminated reactively at end of the dees, but resistively at the end of the resonator stems. An iterative process is used to find the resonance frequency of the circuit, and the circuit properties are then computed at this frequency for a selected maximum dee voltage, thus providing the voltage and current distribution in the resonator as well as approximations for its power consumption and Q-value.

The resonator geometry shown in Figure 1 is based on the results of such a design procedure. The impedances of the transmission-line sections in this representation were calculated using a two-dimensional field analysis code. The acceleration gap increases from 5 mm in the central region to 100 mm at extraction, and provision was made for a 5-fold increase of the dee-voltage over this distance. Figure 3 shows the half-scale model of this resonator which was built to determine its performance experimentally. A resonance frequency of 202 MHz was measured on the model, which is equivalent to 101 MHz at full scale. The slight modification of the resonator geometry needed to reach 106 MHz does not pose a serious problem. The nearest parasitic resonance was excited at 390 MHz.

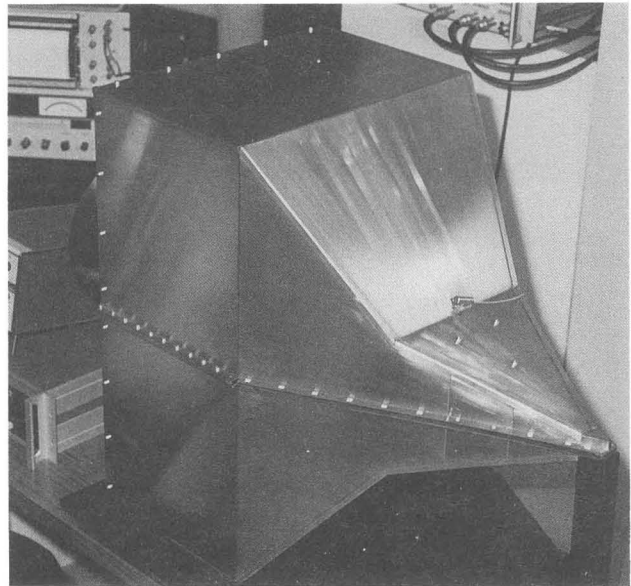


Figure 3: The half-scale resonator model on the test bench.

The measured Q-value of the model is 4000, which would be equivalent to 5500 at full scale, but is much lower than expected originally. A factor of  $\sim 1.8$  of this discrepancy was explained by taking geometrical details and non-uniform current densities on the resonator surfaces into account, while the remaining factor of 2 can be related to the increase in rf-resistance which is caused by the mechanical and microscopic roughness of the copper surfaces. With a Q-value of 5500 the power consumption of the resonator will not exceed 100 kW for a maximum dee voltage of 250 kV.

The radial distribution of the dee voltage at the acceleration gap was determined using measurements with a loosely coupled rf-pickup probe, and is compared with the result of the design calculations in Figure 4. Generally the agreement is good, except in the nose region of the resonator, where the calculated dee voltage increases from the position of the stem connection toward the cyclotron centre, while the measured values keep on falling with decreasing radius. This effect, which cannot be explained without a three-dimensional analysis, would lead to an unacceptably low puller voltage for the ion source and must be corrected till a peak value of  $\geq 40$  kV is attained at the nose of the dee.

#### 5 Expected Beam Characteristics

A cold-cathode ion source, similar to the type proposed at MSU<sup>2</sup> which features a 50 mm high ionisation chimney of 6 mm diameter, should easily provide the beam current ( $< 100$ nA) and brightness required for proton therapy. Assuming a puller voltage of 40 kV and considering the central field of 1.74 tesla, the source is located

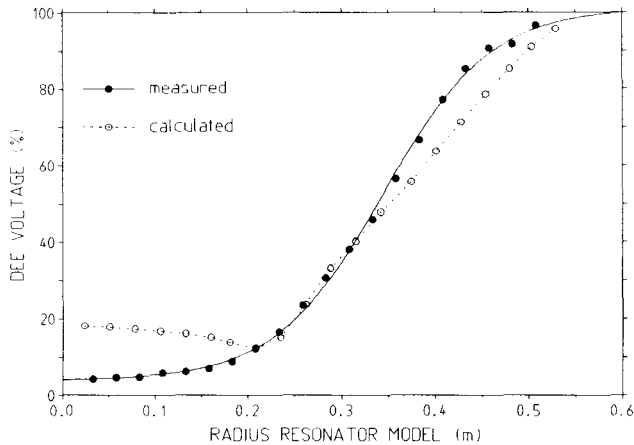


**Figure 4:** The radial dee-voltage distribution at the acceleration gap of the resonator model.

approximately at a radius of 12 mm in the valley preceding the dee with the puller. The acceleration gap between the ion source and the puller can be made  $\geq 5$  mm under these conditions, and the probability of sparks is greatly reduced, thus providing for very stable operation.

The phase width of the beam can be limited to less than  $24^\circ$  (rf) on the first turn by two 1 mm wide radial slits which are separated a quarter turn. Because the radial betatron frequency is close to 1 in this region, the remaining beam should have only a radial emittance of up to  $8\pi$  mm mrad, and will safely bypass the ion source after completing the first turn at a radius of  $\sim 35$  mm. The axial beam emittance can be selected together with the beam current using an adjustable vertical slit after  $\sim 2\frac{3}{4}$  turns at a radius of 50 to 60 mm, and will be in the same order of magnitude as, but probably smaller than the radial emittance, depending on the performance of the ion source. For centering the orbits, either the position of the ion source must be adjustable or a set of first harmonic centering coils has to be provided.

As the protons gain momentum in the SRC, adiabatic damping decreases the initial beam emittances by a factor close to 9 on the 220 MeV orbit, which leads to a full radial beam width of less than 1 mm at extraction. This includes a tail of 0.2 mm due to the energy spread of the beam, which is very small in this machine because the initial phase width will be compressed by a factor 6 to only  $4^\circ$  (rf). With an energy gain of 1 MeV per turn, the orbit separation at 220 MeV is only 1.7 mm, but can easily be increased to  $\geq 4$  mm using a suitable centering error of the orbits. The inherent beam separation is  $\geq 3$  mm under these conditions, and more than adequate to provide clean single-turn extraction with the septum of the electrostatic extraction channel (EEC) shown in Figure 1, as long as the radial position of the beam can be kept sufficiently stable. Radial beam sweeps are caused by mechanical, electric and magnetic instabili-

ties, and should not exceed 1 mm in total, which is equivalent to a sweep amplitude of 0.5 mm. Half of the allowed radial beam sweep is used up by the phase and amplitude stabilities of the rf-system mentioned earlier, while the remaining half makes provision for the other effects.

Beam extraction is facilitated considerably by the small beam size and relatively low guiding field in the valleys ( $< 1.2$  tesla), which allows the efficient use of advanced permanent magnets with a high strength and coercive force, and also makes provision for reliable and stable operational characteristics of the EEC. Small permanent magnets can easily produce the first harmonic field bumps needed for decentering the beam over the last few turns before extraction, and would be mounted on opposite extraction devices, so that they automatically change position for variable-radius extraction. In fact, the centering error could be made much larger in this way with  $v_x \leq 1.4$ , but this may lead to a serious deterioration of the beam quality due to the  $v_x = 4/3$  resonance.

The EEC shown in Figure 1 is a version of the one in our SSC, with a radial field strength up to 10 kV/mm over an azimuthal channel length of 0.4 m. Such an EEC will increase the beam separation to more than 10 mm at the position of the first of the two septum magnets (SPM1), which are located inside a dee and followed by another septum magnet (SPM2) and a bending magnet (BM) or magnetic channel in the extraction valley.

#### Acknowledgements

We would like to thank Mr D.P. Brombach and Mr V. Vranković of the Magnet Section at PSI for their continued support with the TOSCA calculations, as well as Mr M. Webb and his team in our workshop for manufacturing the resonator model so well.

#### References

1. W. Beekman *et al.*, *Nucl. Inst. Meth. B* **56/57**, 1201 (1991).
2. H.G. Blosser *et al.*, *Report MSUCL-874*, MSU, East Lansing MI (1993).
3. P. Mandrillon *et al.*, *Proc. 4th Eur. Part. Acc. Conf.*, Vol. 3, 2604 (1994).
4. E. Acerbi *et al.*, this conference.
5. Y. Jongen *et al.*, this conference.
6. J.B. Flanz *et al.*, this conference.
7. E. Pedroni *et al.*, this conference.
8. H.N. Jungwirth and J.G. de Villiers, *Proc. 13th Int. Conf. on Cycl. and their Applic.* 709 (1992).
9. Vector Fields Ltd, *The Tosca Reference Manual*, Oxford (1994).
10. H.G. Blosser, private communications.